Hetherington, P. J., "Absorption of SO_2 into Aqueous Media: A Mechanism Study," Ph.D. dissertation, Univ. Tasmania (1968).
Horne, R. A., *Marine Chemistry,* Wiley-Interscience, New York (1969).
Hudson, J. C., "The Solubility of Sulfur Dioxide in Water and in Aqueous Solutions of Potassium Chloride and Sodium Sulfate," *J. Chem. Soc. (London),* **79,** 1332 (1925).
Johnstone, H. F., and P. W. Leppla, "The Solubility of SO_2 at Low Partial Pressures. The Ionization Constant and Heat of Ionization of Sulfurous Acid," *J. Am. Chem. Soc.,* **56,** 2233 (1934).
Lewis, G. N., M. Randall, K. S. Pitzer, and L. Brewer, *Thermodynamics,* 2 ed., McGraw Hill, New York (1961).
Latimer, W. M., and H. H. Hildebrand, *Reference Book of Inorganic Chemistry,* 3 ed., The MacMillan Company, New York (1965).
Munjal, P., and P. B. Stewart, "Correlation Equation for Solubility of Carbon Dioxide in Water, Seawater, and Seawater Concentrates, *J. Chem. Eng. Data,* **16,** 170 (1971).
Parkison, R. V., "The Solubility of Sulfur Dioxide in Water and Sulfuric Acid," *TAPPI,* **39,** 517 (1956).
Pearson, D. A., L. A. Lundberg, B. West, and J. L. McCarthy, Absorption on a Semi Works Scale. Absorption of Sulfur Dioxide in a Packed Tower," *Chem. Eng. Prog.,* **47,** 257 (1951).
Plummer, A. W., "Thermodynamic Data for the System SO_2-H_2O. Bibliography and Critical Analysis," *ibid.,* **46,** 369 (1950).
Rabe, A. E., and J. F. Harris, "Vapor Liquid Equilibrium Data for the Binary System, Sulfur Dioxide and Water," *J. Chem. Eng. Data,* **8,** 333 (1963).
Riley, J. P., and G. Skirrow, *Chemical Oceanography,* Vol. 1, 2 ed., Academic Press, New York (1970).
Robinson, R. H., and R. H. Stokes, *Electrolyte Solutions,* 2 revised ed., Butterworths, London, England (1968).
Roy, A., and J. Yahalom, "Protection of Sea Water Desalting Equipment by Oxygen Scavenging, "paper presented at 2nd International Congress on Marine Fouling and Corrosion, Athens, Greece (1968).
Schroeter, L. C., *Sulfur Dioxide,* Pergamon Press, New York (1966).
Seidell, A., *Solubilities of Inorganic and Metal Organic Compounds,* 3 ed., D. Van Nostrand, New York (1940).
Sherwood, T. K., "Solubilities of Sulfur Dioxide and Ammonia in Water," *Ind. Eng. Chem.,* **17,** 745 (1925).
Smith, W. T., and R. B. Parkhurst, "The Solubility of Sulfur Dioxide in Suspensions of Calcium and Magnesium Hydroxides," *J. Am. Chem. Soc.,* **44,** 1918 (1922).
Sridhar, S., "Adsorption of Sulfur Dioxide from Dilute Gases by Seawater in a Packed Column," Ph.D. thesis, Univ. Calif., Berkeley (1975).
Sverdrup, H. U., M. W. Johnson, and R. H. Fleming, *The Oceans. Their Physics, Chemistry and General Biology,* Prentice Hall, Englewood Cliffs, N.J. (1959).
Tartar, H. V., and H. H. Garretson, "The Thermodynamic Ionization Constants of Sulfurous Acid at 25°C," *J. Am. Chem. Soc.,* **63,** 808 (1941).
Thompson, M. E., and J. W. Ross, Jr., "Calcium in Sea Water by Electrode Measurement," *Science,* **153,** 1643 (1966).
Thompson, M. E., "Magnesium in Sea Water: An Electrode Measurement," *ibid.,* 866 (1966).

APPENDIX: TEMPERATURE DEPENDENCE OF THERMODYNAMIC EQUILIBRIUM CONSTANTS*

Values of K_1, the first dissociation constant of sulfur dioxide(aq) at temperatures other than 25°C, were obtained by interpolation on a log K vs. $1/T$ plot. The plot was constructed from the data of Campbell and Maass (1930) who studied K_1 over a temperature range of 5° to 90°C. For K_3, the first dissociation constant of carbon dioxide(aq), and K_5, the second dissociation constant of sulfuric acid, the variation with temperature was estimated from the following correlations reported in Robinson and Stokes (1968):

$$pKH_2CO_3 = \frac{3\,404.71}{T} - 14.8435 + 0.032786T \quad \text{(A1)}$$

$$pKHSO_4^- = \frac{475.14}{T} - 5.0435 + 0.01822T \quad \text{(A2)}$$

The temperature dependence of HSO_2 and HCO_2 was calculated from the following correlations reported by Rabe and Harris (1963) and Munjal and Stewart (1971), respectively:

$$HSO_2 = \exp\left(-\frac{2\,851.1}{T} + 9.3795\right) \quad \text{(A3)}$$

$$HCO_2 = \exp\left(\frac{-2\,734.1}{T} + 16.83\right) \quad \text{(A4)}$$

Equation (A4) uses the mole fraction instead of molality as the concentration unit, and hence the calculated value of HCO_2 must be adjusted to conform to the units used in the model.

Manuscript received March 20, 1976; revision received October 16, and accepted November 5, 1976.

Drop Sizes in Annular Gas-Liquid Flows

The droplets that appear in annular gas-liquid flows are formed by the eruption of wavelets from the surface of the wall layer. Ninety per cent of the volume of this dispersed liquid is carried by only about 10% of the drops. We find, as suggested by Wicks and Dukler, that the distribution of drop sizes can be characterized by an upper limit, log normal function with only one of the three parameters, the volume median diameter, a strong function of flow conditions. A method for predicting the average diameter is suggested which is consistent with a theoretical interpretation based on a Kelvin-Helmholtz mechanism, whereby the destabilizing force is the pressure variation over the wavelets.

DAVID F. TATTERSON
JOHN C. DALLMAN
and
THOMAS J. HANRATTY
University of Illinois
Urbana, Illinois

SCOPE

When a gas and a liquid are transported in a duct with high gas velocities and with a relatively low ratio of liquid to gas throughput, an annular regime exists whereby a liquid layer flows along the wall and a high velocity gas stream flows concurrently. The liquid layer, which has an agitated wavy surface, can be entrained into the gas.

Correspondence concerning this paper should be addressed to Thomas J. Hanratty.

* K_2 was assumed constant with temperature owing to lack of data at temperatures other than 25°C. The variation of K_4 with temperature was not estimated because this equilibrium was neglected in this study. K_w was assumed constant over the temperature range of interest, 10 to 25°C.

This entrained liquid is carried along as droplets with a large range of diameters. The droplets deposit on the wall layer so that the amount of entrained liquid depends on the relative rates of deposition and entrainment, as well as on the entry condition. This paper analyzes data presently available in the literature, as well as some recent measurements made in our own laboratory by Tatterson (1975), in order to suggest a method for predicting drop sizes in such flows.

A function with at least three parameters appears to be needed to fit data on drop size distribution. Wicks and Dukler (1966) recommended an upper limit, log normal distribution (Mugele and Evans, 1951) and suggested that only one of the parameters is a function of the flow variables. We find this scheme to be a convenient method of correlation.

Wicks and Dukler used the maximum diameter d_m to represent droplet size. They suggested that this can be related to the critical diameter above which a droplet will shatter in a flowing stream. From an analysis presented by Hinze (1955), it would then follow that $d_m\rho_G(u_G - u_d)^2/\sigma$ should be constant. However, available data indicate that d_m does not vary with the gas velocity squared.

Consequently, we examine an alternate criterion for characterizing droplet size. On the basis of photographic studies of the atomization process made by Woodmansee and Hanratty (1969), we assume atomization occurs through a Kelvin-Helmholtz mechanism, whereby the destabilizing force is the pressure variation over small wavelets on the wall layer.

CONCLUSIONS AND SIGNIFICANCE

The distribution of drop sizes is described by a volume probability density function $f_v(d_p)$ whereby the fraction of the total volume of the spray occupied by droplets with diameters less than d_p is given by $\int_0^{d_p} f_v dd_p$. Presently available data indicate that f_v can be approximated by an upper limit, log normal function defined by Equation (16), where δ, d_m, $d_{v\mu}$ are parameters. The quantity d_m is the maximum drop size, while $d_{v\mu}$ is the volume median diameter, defined so that droplets with diameters greater than $d_{v\mu}$ occupy 50% of the spray volume. Measurements by Tatterson (1975), Wicks and Dukler (1966), and Cousins and Hewitt (1968) suggest that δ and $d_m/d_{v\mu}$ can be respectively approximated as 0.72 and 2.9. A number density function $f_n(d_p)$ defined so that $\int_0^{d_p} f_n dd_p$ is the fraction of the drops with diameters less than d_p can be calculated from f_v. Plots of density functions f_v and f_n and of the cumulative distribution functions $\int_0^{d_p} f_v dd_p$ and $\int_0^{d_p} f_n dd_p$ are given in Figures 4 and 5. Of particular interest is the observation that 90% of the volume is carried by only about 10% of the drops.

A theoretical analysis based on a Kelvin-Helmholtz mechanism for wave instability indicates that $d_{v\mu}/d_t$ $(\rho_G u_G^2 f_s d_t/2\sigma)^{1/2}$ is a weak function of a flow parameter F, similar to the Martinelli flow parameter, of the type shown in Figure 6. Measurements of $d_{v\mu}$ by Tatterson, by Wicks and Dukler, and by Cousins and Hewitt are consistent with this derivation but are not accurate enough to justify taking into account the influence of F. For the present it is recommended that $d_{v\mu}$ be approximated by

$$\frac{d_{v\mu}}{d_t}\left(\frac{\rho_G u_G^2 f_s d_t}{2\sigma}\right)^{1/2} = 1.6 \times 10^{-2}$$

where the friction factor for a smooth interface f_s may be taken as $f_s = 0.046/Re_G^{0.20}$.

A length mean drop diameter can be defined as $d_{10} = \int_0^{\infty} d_p f_n dd_p$. Although droplet distributions measured by Namie and Ueda (1972) and Pogson, Roberts, and Waibler (1970) did not contain enough of the large drops to calculate $d_{v\mu}$, they were adequate for obtaining d_{10}. From these data we recommend that d_{10} be estimated by

$$\frac{d_{10}}{d_t}\left(\frac{\rho_G u_G^2 f_s d_t}{2\sigma}\right)^{1/2} = 2.4 \times 10^{-3}$$

It is concluded that a Kelvin-Helmholtz instability provides a theoretical explanation for droplet formation in annular gas-liquid flows which is consistent with presently available measurements of drop size and with photographic studies by Woodmansee and Hanratty (1969). According to this interpretation, droplets are formed by the growth of small wavelets on the surface of the wall layer due to a destabilizing force arising from pressure variations in the gas flowing over the wave surface.

MEASUREMENTS OF DROP SIZE IN ANNULAR FLOWS

Drop sizes have been measured in annular flows with a high speed motion picture camera by Russell and Rogers (1972) for air-water flow in a horizontal channel 0.025 m wide, 0.152 m high, and 4.27 m long. Still photography was used by Cousins and Hewitt for upward flow of air and water in a pipe with a 0.0095 m diameter and by Pogson, Roberts, and Waibler (1970) for upward flow of steam and water in a pipe with a diameter of 0.0032 m. Namie and Ueda (1972) measured drop size for air-water flow in a horizontal 0.06 × 0.01 m channel by collecting samples of the spray in a silicone oil.

Wicks and Dukler (1966) and Wicks (1967) developed an electrical conduction probe to measure drop size. Two needles pointing at each other were placed in the air stream containing droplets. When a conducting particle strikes both needles, a current pulse occurs. By varying the spacing between the needle tips, the functionality between the counting rate and distance of separation is determined. The drop size distribution is extracted from these results by numerical methods. Wicks and Dukler used this technique for the downward flow of air and water in a rectangular channel, 0.15 m wide, 0.019 m deep, and 5.49 m long. A discussion of its accuracy has been presented by Pye (1971).

Tatterson (1975) applied the electric probe suggested by Geist et al. (1951) to measure drop sizes for air-water flow in a horizontal rectangular channel 0.025 m deep, 0.305 m wide, and 9.1 m long. A wire charged to a high voltage is placed in a flow stream. When a conducting droplet strikes the probe, its surface charges to the probe's potential, thereby causing a pulse in the external circuit. The signal from the probe is analyzed electrically to get the drop size distribution. Problems were encountered because wetting of the insulated support holding the charged

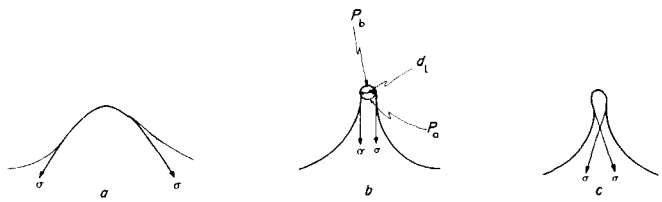

Fig. 1. Kelvin-Helmholtz mechanism for the formation of droplets.

wire can provide a conducting path to the wire. Consequently, more work is required with this technique before it can be used with confidence over a wide range of flow conditions. In this paper we only present measurements made by Tatterson at the inlet region of the channel where entrainment is small and wetting problems are not serious.

CHARACTERIZATION OF DROP SIZE

Mechanism of Drop Formation

At conditions that prevail in annular flow, the interfacial structure of the liquid wall layer is characterized by a series of flow surges, called roll waves, which have a highly agitated surface and which are accompanied by increases in the thickness of the wall layer. Woodmansee and Hanratty (1969) took high speed motion pictures of the liquid wall layer during atomization. The pictures showed a number of mechanisms for droplet removal. These include the splattering of the liquid surface after a droplet impingement and the bursting of air bubbles found chiefly in the roll waves. However, most of the droplet removal was observed to occur by the rapid acceleration, lifting, and subsequent shattering of ripples present in the roll wave surface.

The following sequence of events is described in the article by Woodmansee and Hanratty: "One of these ripples suddenly accelerates and moves toward the front of the roll wave. The central section of the ripple is lifted by the air stream leaving one or both of the ends connected to the flowing thin film. As the detached region of the apparent tube of liquid is lifted, it is blown into an arc which narrows as it stretches downstream until it ruptures in a number of places. Though difficult to count, as many as ten to twenty droplets can be sent streaming off into the flowing air after the filament rupture. Finally, the end still attached to the water film lies down ahead of the roll wave and is swept under the passing disturbance."

This process of droplet formation in annular flow has similarities to what has been observed in swirling atomizers, in droplet disintegration by air streams, and in pneumatic atomizers (Lane and Green, 1956; Marshall, 1954).

For example, Lane and Green (1956) give the following description of the formation of droplets in spinning disk atomizers at low liquid rates: "A liquid torus tends to be formed at the edge, but owing to surface tension, it gathers into beads, uniformly distributed which are flung off the edge . . . . As each drop breaks away it is elongated and, between it and the disk, a connecting ligament is formed which thins down until it is detached from the drop. Subsequently, the ligament draws itself up into an irregularly shaped drop which breaks into two satellites."

Kelvin-Helmholtz Mechanism

In all four of the types of atomization cited above, the large sized droplets carrying most of the mass are formed by the breakup of tubes or ligaments of fluid. A number of authors have indicated that these droplets scale as the diameter of the fluid ligament. For example, Walton and Prewitt (1949) have correlated the measured droplet diameters d_p at low liquid rates in a disk atomizer of diameter D spinning at angular velocity ω by considering the balance between the centrifugal force on the liquid torus before detachment and surface tension σ to conclude that $d_p(D\omega^2\rho_L/\sigma)^{1/2}$ is a constant.

An argument similar to that of Walton and Prewitt can be used in annular two-phase flow. It envisions ligaments of fluid being torn from the crest of wavelets because of an imbalance between the forces due to pressure variation over the wave crest and due to surface tension. Consider the volume of fluid at the crest of the long crested wave shown in Figure 1. Because the gas velocity over the crest is larger than in the trough, the crest experiences a reduced pressure due to a Bernoulli effect. The vertical component of the surface tension force, which acts along the length of the wave crest, opposes this suction. As this volume is deformed into a ligament, the radius of curvature decreases and the vertical component of the surface tension force increases. If these surface tension forces are great enough, they can inhibit further distortion of the crest. However, if the crest distorts to the condition indicated in Figure 1*b*, where the surface tension force is acting vertically, an unstable configuration is reached for which further distortion of the crest would lead to a decreasing importance of surface tension, as shown in Figure 1*c*.

By considering a static force balance for the critical configuration in Figure 1*b*, we get the following criterion for the formation of a ligament diameter d_L:

$$\Delta P\, d_L = 2\sigma \tag{1}$$

where ΔP is the pressure difference between the points a and b. By using Kelvin-Helmholtz theory for the flow of an inviscid fluid over a small amplitude wave, we estimate the pressure gradient as $\rho_G u_G^2 k$ and ΔP as $\rho_G u_G^2 k d_L$, where k is the wave number of the wave producing the ligament. If this estimate for ΔP is substituted into (1), and if it is assumed that the drops formed from the ligament are proportional to the ligament diameter, it follows that

$$d_p \left(\frac{\rho_G u_G^2 k}{\sigma}\right)^{1/2} = \text{constant} \tag{2}$$

It would be expected that the wave number k in (2) could be approximated as that of the fastest growing wave. For wavelets on thick liquid layers, Taylor's (1940) analysis of a Kelvin-Helmholtz instability would give

$$k_m = \frac{\rho_G u_G^2}{\sigma} f(\theta)$$

where

$$\theta = \frac{\rho_L}{\rho_G} \frac{\sigma^2}{\mu_L^2 u_G^2}$$

is a measure of the influence of liquid viscosity. We then get for thick liquid layers that

$$\frac{\rho_G u_G^2 d_p}{\sigma} = f(\theta) \tag{3}$$

where $f(\theta)$ is a weak function of θ. This is similar to the relation that Wicks (1967) obtained by using the criterion of the critical drop diameter in a flowing gas.

However, the wavelets observed to be atomizing in annular flows have wavelengths which are too large relative to the height of the wall layer to be approximated by a deep water analysis. Consequently, the above evaluation of k would not be expected to be valid. From experimental observations, it seems more appropriate to approximate

k by assuming that the wavelength of the unstable wavelets scales as the average height of the wall layer m. This assumption has been supported by calculations of Tatterson (1975) on the growth of waves caused by the pressure and shear forces that an air flow exerts in a liquid surface. He found that in the range of variables of interest in annular flow, the growth rate increased with increasing wavelength. However, if the film height is small enough with respect to the wavelength that the wave motion is described by a shallow water approximation, the growth of the waves is dominated by the shear stress variation over the wave rather than by pressure variation. Tatterson argued that waves for which shear stress dominates will tumble over when they become large enough and that growth must be dominated by the pressure variation for atomization to occur. Consequently, the height of the wall layer tends to regulate the length of the atomizing wavelet.

From the assumption that $k \sim m^{-1}$, it follows that for shallow liquid layers

$$\left(\frac{d_p}{m}\right)\left(\frac{\rho_G u_G^2 m}{\sigma}\right)^{1/2} = \text{constant} \tag{4}$$

The use of (4) requires the specification of an appropriate value for u_G since the analysis was carried out on the assumption that u_G is uniform. The distance over which the influence of a surface disturbance penetrates a flowing stream is proportional to the wavelength. Consequently, the characteristic gas velocity is evaluated at a distance from the interface which is proportional to the wavelength $y = c_1\lambda$. Both Lilleleht and Hanratty (1961) and Gill, Hewitt, and Hitchon (1962) contend that the variation of the gas velocity with distance above the interface is given by

$$\frac{u_G}{u^*} = \frac{1}{\kappa}\ln\frac{y}{\epsilon} + B \tag{5}$$

where

$$u^* = u_G\sqrt{\frac{f_i}{2}} \tag{6}$$

Since the roughness should scale as the wavelength $\epsilon = c_2\lambda$, we suggest that the characteristic velocity to be used in (4) is proportional to the friction velocity

$$\left(\frac{d_p}{m}\right)\left(\frac{\rho_G u^{*2} m}{\sigma}\right)^{1/2} = \text{constant} \tag{7}$$

Recent work by Henstock and Hanratty (1976) has shown that the height of the wall layer and the friction factor f_i can be approximated by the following equations for vertical upflows at large gas velocities:

$$\frac{m}{d_t} = \frac{6.59F}{(1 + 1\,400F)^{1/2}} \tag{8}$$

and

$$\frac{f_i}{f_s} = 1 + 1\,400F \tag{9}$$

where the friction factor for a smooth surface f_s is given by the equation

$$f_s = \frac{0.046}{Re_G^{0.20}} \tag{10}$$

The term F is a flow parameter similar to that proposed by Martinelli

$$F = \frac{\gamma(Re_{LF})}{Re_G^{0.90}}\,\frac{\nu_L}{\nu_G}\sqrt{\frac{\rho_L}{\rho_G}} \tag{11}$$

with

$$\gamma = [(0.707Re_{LF}^{0.50})^{2.5} + (0.0379Re_{LF}^{0.90})^{2.5}]^{0.40}$$

There is some indication that (9) overpredicts friction factors for horizontal flows and that for vertical downflows at relatively low velocities the influence of a gravity group $G = (\rho_L g d_t)/(\rho_G u_G^2 f_s)$ must be taken into account. However, the accuracy of presently available measurements of drop diameter does not justify taking into account these secondary influences of the orientation of the tube on f_i.

These relations developed by Henstock and Hanratty suggest that we write (7) as

$$\left(\frac{d_p}{d_t}\right)\left[\frac{\rho_G u_G^2\left(\frac{f_s}{2}\right)d_t}{\sigma}\right]^{1/2} = c_3\left(\frac{m}{d_t}\right)^{1/2}\left(\frac{f_s}{f_i}\right)^{1/2} \tag{12}$$

where c_3 is a proportionality constant. Equation (12) is plotted in Figures 6 and 7 using the relations (8) and (9) developed by Henstock and Hanratty. From these plots, we conclude that the theory developed in this section implies that we characterize the drop diameter by

$$\left(\frac{d_p}{d_t}\right)\left[\frac{\rho_G u_G^2\left(\frac{f_s}{2}\right)d_t}{\sigma}\right]^{1/2}$$

and that this group should be a relatively weak function of flow parameter F over the range of interest for annular flow in small diameter pipes.

Taylor's Kelvin-Helmholtz Mechanism

The results presented in the previous section differ from the results obtained by Taylor (1940) in his paper on the generation of drops due to a Kelvin-Helmholtz mechanism in that Taylor assumed the droplets scale as the wavelength of the unstable wave rather than as the diameter of the ligament removed from the wave crest. For deep liquid layers, the two approaches give the same result, Equation (3). However, for shallow layers Taylor's assumption would give a result quite different from (4); that is

$$\frac{d_p}{m} = \text{constant} \tag{13}$$

DROPLET DISTRIBUTION FUNCTION

Excellent reviews of the distribution functions used to represent drop sizes observed in atomization processes have been given by Mugele and Evans (1951) and by Marshall (1954). Quite often, as is the case for annular flows, it is not convenient to measure the number distribution function f_n because the large number of very fine particles present makes it difficult to measure the total number of particles. In such cases, a normalized volume distribution function may be used. It is defined as

$$\frac{dv}{dd_p} = f_v(d_p) \tag{14}$$

$$\int_0^\infty f_v(d_p)\,dd_p = 1 \tag{15}$$

and it gives the fraction of the volume made up of particles between d_p and $d_p + dd_p$. Since the volume of a particle varies as d_p^3, we can see that the larger particles are contributing much more to the total volume than smaller particles. The volume distribution function is skewed more in the direction of large d_p than is the number distribution function, and the volume median diameter $d_{v\mu}$ is considerably larger than the number median diameter $d_{n\mu}$.

The upper limit, log normal distribution used by Mugele

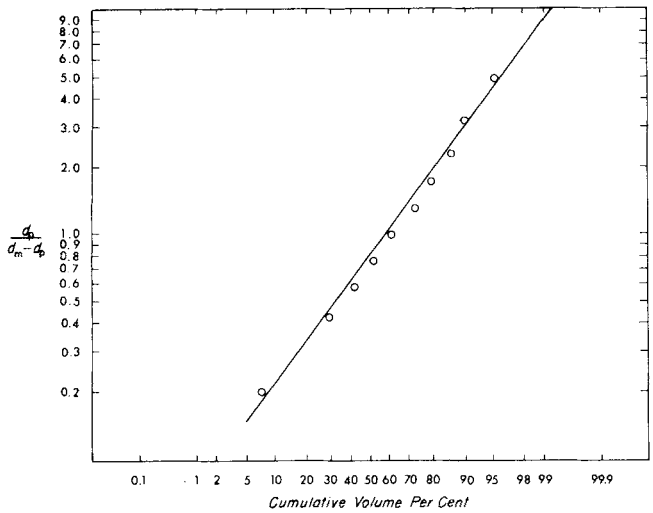

Fig. 2. Example of upper limit, log normal distribution.

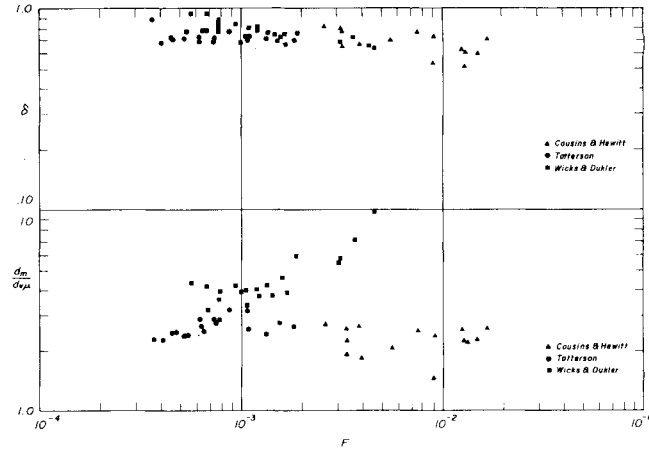

Fig. 3. Measurements of parameters used in upper limit, log normal distributions.

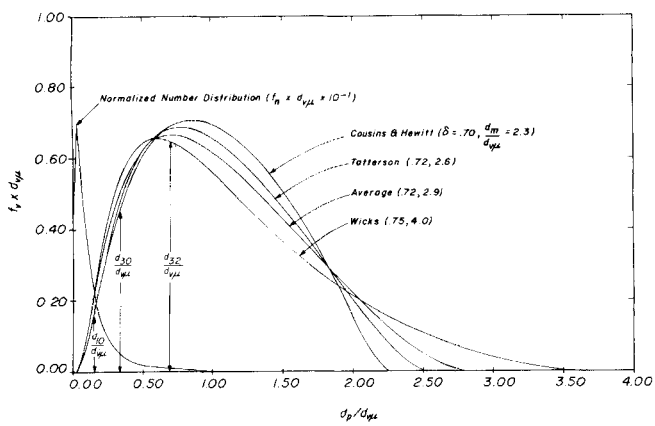

Fig. 4. Volume probability density functions and average normalized number distribution.

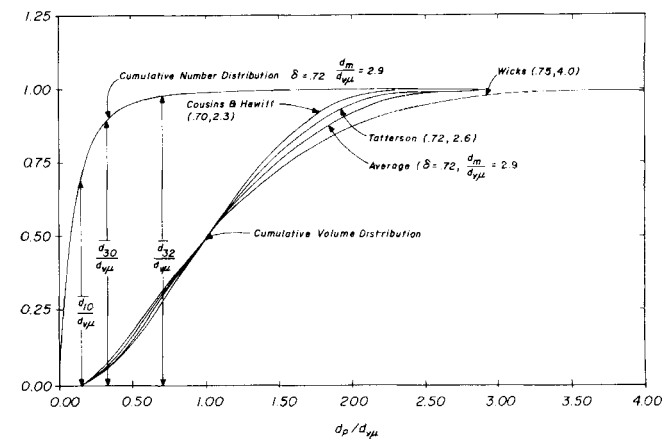

Fig. 5. Cumulative number and volume distributions.

and Evans (1951) for atomizing jets and by Wicks and Dukler (1966) for annular flow can be written in the following form:

$$\frac{dv}{dd_p} = \frac{\delta d_m}{\sqrt{\pi}\, d_p(d_m - d_p)} \exp\left[-\delta^2\left(\ln\frac{d_p}{d_m - d_p} - \ln a\right)^2\right] \tag{16}$$

We have chosen to characterize this distribution function by the three parameters $d_{v\mu}$, $d_m/d_{v\mu}$, and δ. The quantity a appearing in (16) is then given by

$$a = \frac{d_{v\mu}}{d_m - d_{v\mu}} \tag{17}$$

Mugele (1960) found δ to depend only on the type of atomizer used to generate sprays, and from the results presented by Wicks and Dukler (1966), it would be expected that δ and $d_m/d_{v\mu}$ would be only weakly dependent on flow variables for annular flows.

The characterization of the droplet size with the volume median diameter is not unique. Another possible choice would be one of average particle diameters $\overline{d}_{qm}$, defined by Mugele and Evans (1951), where

$$\overline{d}_{qm}^{m-n} \int_0^\infty d^m f_n dd_p = \int_0^\infty d^q f_n dd_p \tag{18}$$

If $d_m/d_{v\mu}$ and δ are independent of flow parameters, then $\overline{d}_{qm}/d_{v\mu}$ is constant and the relations developed in the previous section would be applicable both for $d_{v\mu}$ and $\overline{d}_{qm}$.

CORRELATION OF MEASUREMENTS

Drop Size Distribution

Only the drop size measurements of Tatterson, of Cousins and Hewitt, and of Wicks and Dukler had a large enough sample size that a volume distribution function could be accurately determined. They were fitted to an upper limit, log normal distribution by selecting a value of d_m such that a plot of the cumulative volume per cent of liquid with drops less than d_p vs. $d_p/(d_m - d_p)$ on log probability graph paper should produce a straight line. A typical example of such a fit is shown in Figure 2 for one of the runs of Tatterson.

Values of δ and $d_{v\mu}/d_m$ determined from the distributions of Tatterson, of Cousins and Hewitt, and of Wicks and Dukler are compared in Figure 3, where the change of flow conditions is characterized by the flow parameter F. It is to be noted that δ and $d_{v\mu}/d_m$ are approximately independent of flow conditions as suggested by Wicks and Dukler. However, the values of these parameters determined from the three investigations are not the same, probably because of differences in the techniques used to measure drop size. The volume probability density and cumulative distribution functions calculated from the average values of δ and $d_m/d_{v\mu}$ are plotted in Figures 4 and 5.

Table 1. Average Drop Diameters Calculated from the Upper Limit, Log Normal Distribution for $\delta = 0.72$ and $d_m/d_{v\mu} = 2.9$

$\frac{\overline{d}_{10}}{d_{v\mu}} = 0.15$	$\frac{\overline{d}_{21}}{d_{v\mu}} = 0.37$
$\frac{\overline{d}_{20}}{d_{v\mu}} = 0.24$	$\frac{\overline{d}_{31}}{d_{v\mu}} = 0.76$
$\frac{\overline{d}_{30}}{d_{v\mu}} = 0.34$	$\frac{\overline{d}_{32}}{d_{v\mu}} = 0.70$
$\frac{\overline{d}_{40}}{d_{v\mu}} = 0.45$	$\frac{\overline{d}_{43}}{d_{v\mu}} = 1.04$

The curve representing a composite of the results from the three laboratories is calculated from values of $\delta = 0.72$ and of $d_m/d_{v\mu} = 2.90$.

The number probability density function and the number cumulative distribution function calculated from the composite volume distribution function are also shown in Figures 4 and 5. Values of $d_{10}/d_{v\mu}$, $d_{30}/d_{v\mu}$, and $d_{32}/d_{v\mu}$ calculated from the composite distribution are given in Table 1 and indicated in Figures 4 and 5. Of particular interest is the result that the bulk of the fluid is carried by a small fraction of the drops. For example, as can be seen in Figure 5, drops with diameters less than the length mean $\overline{d}_{10}$ occupy only 1% of the volume.

Volume Median Diameter

Values of the volume median diameter determined from the measurements of Tatterson, of Cousins and Hewitt, and of Wicks and Dukler are summarized in Tables 2, 3, and 4. It is seen that they are not consistent with the assumption that the volume median diameter scales as the wavelength of the unstable waves, since $d_{v\mu}/m$ is not constant. Likewise, the notion that the large sized droplets are governed by droplet stability in a flowing air stream does not appear to correlate available data in that the Weber number based on the volume median diameter $(\rho_G u_G^2 d_{v\mu})/(\sigma)$ is not constant.

A closer examination of all of the data reveals that $d_{v\mu}$ is a weaker function of gas velocity than would be indicated by the criterion of a constant Weber number. In fact, presently available data are more consistent with the condition

$$\left(\frac{d_{v\mu}}{d_t}\right)\left[\frac{\rho_G u_G^2 \frac{f_s}{2} d_t}{\sigma}\right]^{1/2} = \text{constant} \cong 1.6 \times 10^{-2} \tag{19}$$

as shown in Figure 6. This plot gives measurements obtained in three different geometries: upward flow in a pipe, horizontal flow in a rectangular channel, and downward flow in a rectangular channel. Some variability is observed in the above group in each set of data shown in Figure 6. However, no systematic influence of any of the flow variables could be detected. Consequently, we conclude that this variability is within experimental error. Although some influence of geometry should be expected, the accuracy of presently available measurements does not seem to justify taking this into account. Consequently, we chose (19) to represent the measurements from all three laboratories, where the constant is an arithmetic average of all the data shown in Figure 6.

Length Mean Diameter

The distributions measured by Namie and Ueda and by Pogson, Waibler, and Roberts did not include enough large sized droplets to determine a volume median diameter. However, they did include enough small diameter droplets to determine the length mean diameters $\overline{d}_{10}$ shown in Figure 7. The influence of system variables on $\overline{d}_{10}$ is represented quite well by the relation

$$\left(\frac{\overline{d}_{10}}{d_t}\right)\left[\frac{\rho_G u_G^2 \frac{f_s}{2} d_t}{\sigma}\right]^{1/2} = 2.4 \times 10^{-3} \tag{20}$$

Table 2. Drop Size Measurements of Tatterson

W_G, kg/s	W_L, kg/s	$\frac{m}{d_t} \times 10^3$	$d_{v\mu}$, μm	$\frac{\rho_G u_G^2 d_{v\mu}}{\sigma}$	$\left(\frac{d_{v\mu}}{d_t}\right) \times 10^2$	$\frac{d_{v\mu}}{m}$
0.303	0.030	2.15	460	7.97	1.35	4.59
0.303	0.041	2.79	460	7.97	1.35	3.54
0.303	0.056	3.65	510	8.84	1.49	3.00
0.303	0.082	5.15	590	10.2	1.73	2.46
0.363	0.030	1.93	630	15.8	2.18	7.01
0.363	0.041	2.58	610	15.3	2.11	5.07
0.363	0.057	3.43	640	16.0	2.21	4.00
0.242	0.057	3.64	480	5.33	1.15	2.83
0.242	0.082	5.15	500	5.56	1.20	2.08
0.242	0.109	6.87	530	5.89	1.27	1.66
0.242	0.135	8.37	590	6.56	1.41	1.51
0.423	0.030	1.72	650	22.1	2.58	8.11
0.423	0.041	2.25	720	24.5	2.85	6.87
0.423	0.057	3.00	620	21.1	2.46	4.44
0.484	0.030	1.61	720	32.0	3.22	9.60
0.484	0.041	2.15	680	30.2	3.04	6.79
0.544	0.030	1.61	660	37.2	3.28	8.80

0.025 m by 0.305 m horizontal flow channel
$d_t = 0.047$ m
fluid pair: air-water

Table 3. Drop Size Measurements of Cousins and Hewitt

W_G, kg/s	W_L, kg/s	$\frac{m^*}{d_t} \times 10^2$	$d_{v\mu}$, μm	$\frac{\rho_G u_G^2 d_{v\mu}}{\sigma}$	$\left(\frac{d_{v\mu}}{d_t}\right) \times 10^2$	$\frac{d_{v\mu}}{m}$
				$\left[\frac{\rho_G u_G^2 \frac{f_s}{2}}{\sigma}\right]^{1/2}$		
0.0050	0.0067	1.23	115	2.37	0.898	1.49
0.0050	0.0120	1.61	203	4.20	1.59	1.91
0.0050	0.0121	1.61	162	3.47	1.27	1.51
0.0050	0.0192	1.91	125	2.58	0.978	0.95
0.0050	0.020	1.94	155	3.19	1.21	1.16
0.0050	0.0204	1.95	156	3.22	1.22	1.15
0.0050	0.0250	2.10	197	4.06	1.54	1.32
0.0050	0.028	2.21	161	3.33	1.26	1.01
0.0088	0.0043	0.794	70.2	4.43	0.907	1.57
0.0088	0 0066	0.911	80.3	3.80	0.898	1.51
0.0088	0 0066	0.911	69.5	5.88	1.04	1.31
0.0088	0.0067	0.922	89.0	5.62	1.15	1.65
0.0088	0.0085	0.989	70.1	4.43	0.906	1.19
0.0088	0.0088	1.01	82.0	5.18	1.06	1.36
0.0088	0.0190	1.44	98.0	6.22	1.27	1.04

0.0095 m diameter vertical upflow tube
$d_t = 0.0095$ m
fluid pair: air water

* Calculated from correlation $\frac{m}{d_t} = \frac{6.59\,F}{(1 + 1\,400\,F)^{1/3}}$

Table 4. Drop Size Measurements of Wicks and Dukler

W_G, kg/s	W_L, kg/s	$\frac{m}{d_t} \times 10^3$	$d_{v\mu}$, μm	$\frac{\rho_G u_G^2 d_{v\mu}}{\sigma}$	$\left(\frac{d_{v\mu}}{d_t}\right) \times 10^2$	$\frac{d_{v\mu}}{m}$
				$\left[\frac{\rho_G u_G^2 \frac{f_s}{2}}{\sigma}\right]^{1/2}$		
0.128	0.063	2.40	394	8.62	1.55	4.86
0.146	0.063	1.95	396	11.3	1.72	6.01
0.173	0.063	2.30	304	12.3	1.57	3.91
0.207	0.063	1.13	257	14.8	1.56	6.73
0.241	0.063	0.976	213	16.7	1.48	6.46
0.292	0.063	0.902	148	17.1	1.23	4.85
0.109	0.126	4.58	389	6.18	1.32	2.51
0.136	0.126	4.05	389	9.87	1.66	2.84
0.174	0.126	1.95	352	14.4	1.83	5.34
0.80	0.189		254	2.15	0.64	
0.088	0 202	7.95	239	2.46	0.67	0.89
0.105	0.202	6.30	282	4.15	0.91	1.32
0.148	0 202	4.00	349	10.3	1.57	2.58
0.165	0.202	3.16	353	12.8	1.75	3.30
0.254	0 202	0.902	227	19.7	1.66	7.45
0.298	0 202	1.01	160	19.1	1.35	4.69
0.095	0.315	6.68	285	3.43	.86	1.26
0.136	0.315	4.64	303	7.47	1.26	1.93
0.171	0.315	3.61	464	18.2	2.37	3.80
0.224	0.315	1.88	256	17.1	1.67	4.03
0.275	0.315	0.902	167	17.0	1.31	5.48
0.119	0.504	6.62	534	10.1	1.96	2.39
0.145	0.504	5.12	660	18.6	2.91	3.81
0.195	0.504	4.35	511	26.1	2.94	3.48
0.261	0.504	1.80	356	32.4	2.66	5.85

0.15 m × 0.0019 m vertical downflow channel
$d_t = 0.0338$ m
fluid pair: air-water

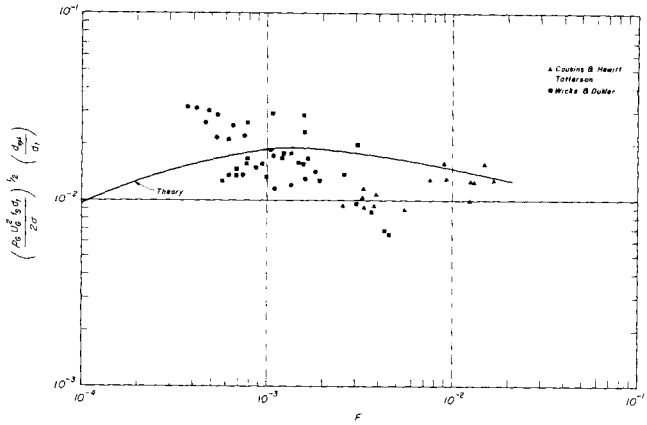

Fig. 6. Comparison of pressure model for vertical upward case with data.

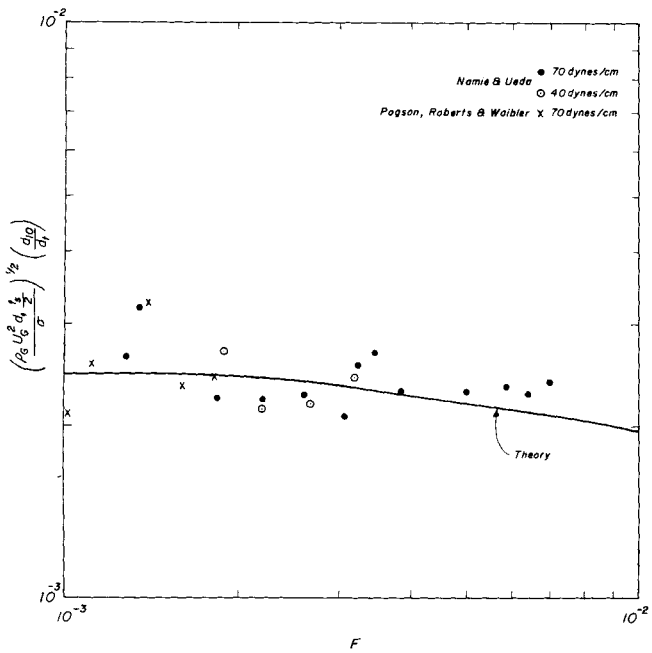

Fig. 7. Pressure model using length mean.

where the constant is determined as an arithmetic average of all the data points. The composite distribution ($\delta = 0.72$, $d_m/d_{v\mu} = 2.90$) shown in Figure 4 gives $\overline{d}_{10}/d_{v\mu} = 0.15$. It is to be noted that (19) and (20) are in exact agreement with this result. The proposed equations for estimating the droplet distribution, the volume median diameter, and the length mean diameter are thus found to be consistent.

Again, it should be pointed out that the sets of measurements shown in Figure 7 were obtained with two different geometries, upflow in a pipe and horizontal flow in a rectangular channel. The close agreement between the two sets of measurements would indicate that the drop size is not very sensitive to the flow orientation.

INTERPRETATION

Two alternate criteria for characterizing drop size than the notion of a critical diameter were considered. One is the Kelvin-Helmholtz mechanism already discussed. The other is the stripping mechanism suggested by Taylor (1940), whereby wavelets are removed because of the shear stress exerted by the gas on the liquid interface. As shown in a thesis by Tatterson (1975), the stripping mechanism does a poor job in predicting the influence of flow variables on drop size. However, a stronger argument for ruling out the stripping mechanism is that it predicts the drop diameter is dependent on liquid viscosity. A comparison of the number mean diameters measured by Pogson and Roberts and by Namie and Ueda for liquid viscosities of 0.28 nN · s/m² and 1.0 $\frac{\text{mN} \cdot \text{s}}{\text{m}^2}$ would suggest a very small influence of this liquid property. Furthermore, Chang (1973) repeated Russell and Rogers' measurements of drop size distributions for the air-water system using two different glycerine-water solutions and found no appreciable influence of liquid viscosity.

According to the Kelvin-Helmholtz mechanism for thin liquid layers, the group $\left(\frac{d_p}{d_t}\right)\left(\frac{\rho_G u_G^2 (f_s/2)\, d_t}{\sigma}\right)^{1/2}$ should be directly proportional to $\left(\frac{m}{d_t}\right)^{1/2}\left(\frac{f_s}{f_i}\right)^{1/2}$, where d_p may either be the volume median diameter $d_{v\mu}$ or the length averaged diameter $\overline{d}_{10}$. This relation is compared with measurements in Figures 6 and 7 using (8) and (9) and proportionality constants of $c_3 = 0.42$ and 0.58. The theory agrees quite well with measurements of $\overline{d}_{10}$ shown in Figure 7 in that it predicts a small influence of F on the group proposed to characterize droplet diameter. It is also consistent with the measurements of $d_{v\mu}$, which show a much larger spread due to experimental error. The agreement in Figure 7 is particularly encouraging since the experiments cover surface tensions of 70 and of 40 mN/m and liquid viscosities from 1 to 0.28 $\frac{\text{mN} \cdot \text{s}}{\text{m}^2}$

It is concluded that the Kelvin-Helmholtz mechanism, as outlined in this paper, provides a theoretical explanation for droplet formation in annular gas-liquid flows which is consistent with presently available measurements of drop size and with photographic studies made by Woodmansee and Hanratty (1969). Drop size measurements with a larger range of equipment sizes and of fluid properties would, however, be desirable in order to test further this proposed mechanism and the method outlined to predict droplet size.

It is to be noted that less variability is found in the measurements of $\overline{d}_{10}$ than in the measurements of $d_{v\mu}$ and d_m. This can be explained since $d_{v\mu}$ and d_m are influenced by the largest sized drops which represent a very small fraction of the total drops sampled. Unless a very large sample is taken, considerable error can therefore be experienced in measuring $d_{v\mu}$ and d_m. This would suggest that the proposed correlation for drop size is more easily tested by measuring $\overline{d}_{10}$ than $d_{v\mu}$.

ACKNOWLEDGMENT

This work was supported by the National Science Foundation under Grant NSF ENG 71-02362 and by the American Institute of Chemical Engineers under the auspices of the Design Institute for Multiphase Processing.

NOTATION

- a = parameter used in upper limit log-normal distribution $a = d_{v\mu}/d_v - d_{v\mu}$
- A = cross-sectional area of the channel
- c_i = proportionality constants
- d_L = diameter of a ligament
- d_m = maximum diameter which appears in the upper limit, log normal distribution
- d_p = diameter of a droplet
- d_t = hydraulic diameter of the channel

$d_{v\mu}$ = volume median diameter; that is, droplets having diameters greater than this occupy half of the spray volume

d_{10} = length mean diameter

$\overline{d}_{qm}$ = generalized particle diameter, defined as (q and m integers)

$$(\overline{d}_{qm})^{q-m} \int_0^\infty d^m f_n \, dd_p = \int_0^\infty d^q f_n \, dd_p$$

D = diameter of a spinning disk atomizer

f_i = gas phase friction factor based on interfacial shear

$$f_i = \tau_i / \tfrac{1}{2}\rho_G u_G^2$$

f_n = normalized number distribution function, where

$$\int_0^{d_p} f_n dd_p$$

is the fraction of the particles with diameter less than d_p

f_s = interfacial friction factor for a smooth surface

f_v = normalized volume distribution function, where

$$\int_0^{d_p} f_v dd_{pp}$$

is the fraction of the volume occupied by particles with diameters less than d_p

F = dimensionless group containing flow rates and fluid properties,

$$F = \frac{\gamma(Re_{LF})}{Re_G^{0.90}} \frac{\nu_L}{\nu_G} \sqrt{\frac{\rho_L}{\rho_G}}$$

g = acceleration of gravity

G = gravity group in friction factor correlation

k = wave number $= 2\pi/\lambda$

k_m = wave number of fastest growing wave

m = thickness of wall layer

n = number of particles

p = channel perimeter

P = pressure

Re_G = Reynolds number of the gas flowing alone in the channel based on hydraulic diameter

Re_{LF} = Reynolds number of the liquid flowing in the wall layer, $Re_{LF} = 4W_{LF}/\mu_L p$

u^* = friction velocity $u^* = (\tau_i/\rho)^{1/2}$

u_d = velocity of a drop

u_G = velocity of the gas $u_G = W_G/\alpha A \rho_G$

v = normalized volume of droplet in distribution

W_G = mass flow rate of the gas in units of mass per unit time

W_L = mass flow rate of the liquid in units of mass per unit time

W_{LF} = mass flow rate of liquid in the wall layer

y = distance from the average level of the interface

Greek Letters

α = void fraction per cent of the area occupied by the gas

$\gamma = \gamma(Re_{LF}) = (0.707 Re_{LF}^{0.50})^{2.5} + (0.0379 Re_{LF}^{0.90})^{2.5\ 0.40}$

δ = parameter in upper limit, log normal distribution

$$\delta = 0.707/\sigma$$

$$\sigma = \ln\left(\frac{\xi_{84\%}}{\xi_{50\%}}\right)$$

ϵ = size of equivalent sand roughness

θ = viscosity number, $\theta = \frac{\rho_L}{\rho_G} \frac{\sigma^2}{\mu_L^2 u_G^2}$

κ = von Karman constant

λ = wavelength

μ = dynamic viscosity

ν = kinematic viscosity $\nu = \mu/\rho$

$\xi_{84\%}$ = value of $d_p/d_m - d_p$ below which 84% of droplet volume lies

$\xi_{50\%}$ = similar to $\xi_{84\%}$

ρ_G = gas density

ρ_L = liquid density

σ = surface tension

ω = rotational speed of a disk atomizer

LITERATURE CITED

Chang, D. R. C., "The Generation, Movement and Deposition of Droplets in Annular Two-Phase Flow," Ph.D. thesis, Univ. Del., Newark (1973).

Cousins, L. B., and G. F. Hewitt, "Liquid Phase Mass Transfer in Annular Two-Phase Flow: Droplet Deposition and Liquid Entrainment," *AERE-R5657* (1968).

Geist, J. M., J. L. York, and G. G. Brown, "Electronic Spray Analysis for Electrically Conducting Particles," *Ind. Eng. Chem.*, **43**, 1371 (1951).

Gill, L. E., G. F. Hewitt, and J. W. Hitchon, "Sampling Probe Studies of the Gas Core in Annular Two-Phase Flow: Part I, The Effect of Length on Phase and Velocity Distribution," *AERE-R3954* (1962).

Henstock, W. H., and T. J. Hanratty, "Interfacial Drag and Film Height in Annular Flows," *AIChE J.*, **22**, 990 (1976).

Hinze, J. O., "Fundamentals of the Hydrodynamic Mechanism of Splitting and Dispersion Processes," *AIChE J.*, **1**, 289 (1955).

Lane, W. R., and H. L. Green, "The Mechanics of Drops and Bubbles," in *Surveys in Mechanics*, Cambridge Univ. Press, London, England (1956).

Lilleleht, L. V., and T. J. Hanratty, "Relation of Interfacial Stress to Wave Height for Concurrent Air-water Flow," *AIChE J.*, **7**, 548 (1961).

Marshall, W. R., "Atomization and Spray Drying," *Chem. Eng. Progr. Monograph Ser.*, **2**, 50 (1954).

Mugele, R. A., "Maximum Stable Droplets in Dispersoids," *AIChE J.*, **6**, 3 (1960).

———, and H. D. Evans, "Droplet Size Distribution in Sprays," *Ind. Eng. Chem.*, **43**, 1317 (1951).

Namie, S., and T. Ueda, "Droplet Transfer in Two-phase Annular Mist Flow," *Bull. J.S.M.F.*, **15**, 1568 (1972).

Pogson, J. T., J. H. Roberts, and P. J. Waibler, "An Investigation of the Liquid Distribution in Annular-mist Flow," *J. Heat Mass Transfer*, **92**, 65 (1970).

Pye, J. W., "Droplet Size Distribution in Sprays Using Pulse-counting Technique," *J. Inst. Fuel*, **44**, 253 (1971).

Russell, T. W. F., and R. W. Rogers, "Droplet Behavior in Horizontal Gas-liquid Flow," presented at AIChE Meeting, Dallas, Tex. (Feb. 20-23, 1972).

Tatterson, D. F., "Rates of Atomization and Drop Size in Annular Two-Phase Flow, "Ph.D. thesis, Univ. Ill., Urbana (1975).

Taylor, G. I., Generation of Ripples by Wind Blowing Over a Viscous Fluid, "The Scientific Papers of Sir Geoffrey Igram Taylor," G. K. Batchelor, ed., Vol. III, Cambridge Univ. Press, London, England (1963).

———, The Shape and Acceleration of a Drop in a High-speed Air Stream, *ibid.* (1963).

Walton, W. H., and W. C. Prewett, "The Production of Sprays and Mists of Uniform Drop Size by Means of Spinning Disc Type Sprayers," *Proc. Phys. Soc.*, **62**, 23 (1949).

Wicks, M., and A. E. Dukler, "In Situ Measurements of Drop Size Distribution in Two-Phase Flow: A New Method for Electrically Conducting liquids," paper presented at International Heat Transfer Conference, Chicago, Ill. (1966).

Wicks, M., "Liquid Film Structure and Drop-Size Distribution in Two-Phase Flow," Ph.D. thesis, Univ. Houston, Tex. (1967).

Woodmansee, D. E., and T. J. Hanratty, "Mechanism for the Removal of Droplets from a Liquid Surface by a Parallel Air Flow," *Chem. Eng. Sci.*, **24**, 299 (1969).

Manuscript received April 23, 1976; revision received September 20, and accepted November 8, 1976.